

Parallelized unscented Kalman filters for carrier recovery in coherent optical communication systems

JOKHAKAR JIGNESH,^{1,*} BILL CORCORAN,^{1,2} ARTHUR LOWERY^{1,2}

¹Monash Electro-Photonics Laboratory, Dept. of Electrical and Computer Systems Engineering, Monash University, Clayton, VIC 3800, Australia

²Centre for Ultrahigh-bandwidth Devices for Optical Systems (CUDOS), Australia

*Corresponding author: jignesh.jokhakar@monash.edu

We show that the unscented Kalman filters (UKF) can be used to mitigate local oscillator phase noise and to compensate carrier frequency offset in coherent single carrier optical communication systems. A parallel processing architecture implementing the unscented Kalman filter is proposed and compared with a previous parallelized linear Kalman filter (LKF), for QPSK and 16-QAM modulation formats. The proposed algorithm is experimentally verified to consume 60% of the processing time compared with the parallelized LKF and simultaneously has a 1.2-dB and 0.8-dB OSNR advantage at the hard FEC limit for QPSK and 16-QAM signals respectively. We experimentally demonstrate these processing algorithms in an 800-km fiber optic transmission link, and similar benefits were observed.

OCIS codes: (060.1660) Coherent communications; (060.2330) Fiber optics communications.

Coherent detection in optical communication systems has allowed for both expanded capacity through access to complex optical modulation formats, and greater reach through the ability to mitigate signal transmission impairments [1]. Coupled with digital signal processing techniques at the receiver, chromatic dispersion and polarization mode dispersion can be largely compensated for [2]. In addition to the compensation of these impairments, signal-processing solutions are required for carrier recovery, which compensates for frequency offset (FO) between the signal carrier and the receiver local oscillator, as well as random phase noise (PN) due to phase drifts between the finite line width lasers.

Carrier recovery techniques can be broadly split into two categories: 'blind' and 'aided' techniques. Blind carrier recovery uses known intrinsic properties of the transmitted signal. A common example for quadrature-phase-shift-keyed (QPSK) signals is the Viterbi-Viterbi algorithm, which can be used for phase noise compensation and frequency offset estimation [3]. A weighted version of Viterbi-Viterbi algorithm has been proposed that uses a Weiner filter to update the weights [4]; however, since the statistical properties of the phase noise vary with time, Weiner filters do not give optimum estimates. For higher order quadrature-amplitude modulation (QAM), different recovery algorithms need to be employed using, for example, radial decision-directed methods [2]. Decision-directed maximum-

likelihood-based estimators [5] require perhaps the least drastic reconfiguration when adjusting to different modulation formats, at the cost of computational complexity. Aided techniques, on the other hand, use an overhead to data in the form of pre-defined preambles, pilot symbols or pilot frequency tones to allow for frequency estimation and phase tracking, sacrificing some bandwidth efficiency [6-8].

As an alternative to these techniques, Kalman filter is a 'blind' technique for carrier recovery. Kalman filters can use a simple ' slicer' [9] for decision-directed operation, with the slicer providing similar modulation format flexibility to maximum-likelihood techniques, but with considerably lower complexity. Moreover, Kalman filters have been shown to converge faster than LMS or CMA algorithms [9], and as an unbiased estimation technique [10], can minimize output signal variance towards an optimal minimum mean-squared error [9]. However, the improvement in performance that Kalman filters provides comes at the cost of increased computational complexity, which can result in unwanted latency in optical communication systems.

Recently, Takashi and Namiki proposed a parallelized architecture implementing a linear Kalman filter (LKF) to perform carrier recovery [11], with parallelization used to improve computation speeds towards those needed for real-time implementation. In this paper, we propose an improved Kalman filtering system, using a parallelized architecture to implement an unscented Kalman filter (UKF) [9]. While UKFs in a serial architecture require more computational effort than LKFs, by exploiting parallelization in parallel architecture, we show that UKFs can outperform LKFs in terms of computation time while concurrently increasing system performance. We show that our proposed parallelized UKF gives a 1.2-dB and 0.8-dB improvement in required OSNR for QPSK at the 7% hard FEC (RS 255, 239) limit over the parallelized LKF for QPSK and 16-QAM modulated signals respectively, and at the same time needs only 60% of the computation time of parallelized LKF. Moreover, by comparing performance of the candidate Kalman filters on both QPSK and 16-QAM modulated signals, we show that our proposed UKF can function with higher-order QAM modulation without drastic changes to the system. The proposed algorithm was also tested in an 800-km fiber optic transmission system, and showed similar performance when using either a UKF or a LKF.

In parallelized implementations of both the UKF and LKF, the received sampled signal is divided into fixed-length blocks. Every sample in each block is processed in parallel by the Kalman filter to get

the estimate of the slope of the phase mismatch in k^{th} block (ω_k) and the value of mismatch at the midpoint of k^{th} block (θ_k). Thus, the state parameter vector to be estimated by the Kalman filters is $x_k = [\theta_k \ \omega_k]^T$. The estimated phase mismatch at each sample in the block as shown in Fig. 1 is then calculated using equation (3).

$$\phi_{n,k} = \theta_k + \left(m - \frac{N+1}{2}\right) \omega_k \quad (3)$$

where, $\phi_{n,k}$ is the phase mismatch at m^{th} sample of k^{th} block, with each block having a length N . Thus, in parallelized case, the Kalman filter algorithm runs once per block instead on every sample in the case of sample-by-sample (serial) architecture.

In the case of the parallelized LKF proposed by Inoue and Namiki [11], the state update equations are

$$\theta_{k+1} = N \cdot \omega_k + \theta_k \quad \text{and} \quad \omega_{k+1} = \omega_k + n_f \quad (1)$$

where N is the block length. The quantity n_f denotes the ‘process noise’ (i.e. change in mismatch slope) between consecutive blocks. The observation model considered in case of LKF is [11]

$$\tilde{\theta}_k = \theta_k + n_\theta \quad \text{and} \quad \tilde{\omega}_k = \omega_k + n_\omega \quad (2)$$

where $\tilde{\theta}_k$ and $\tilde{\omega}_k$ are the actual values for phase mismatch midpoint and slope, and n_θ and n_ω are the observation noises (i.e. prediction errors) associated with these state parameters. To accurately estimate the phase mismatch, the Kalman filtering algorithm attempts to minimize the observation noises (n_θ and n_ω). These quantities are illustrated graphically in Fig. 1.

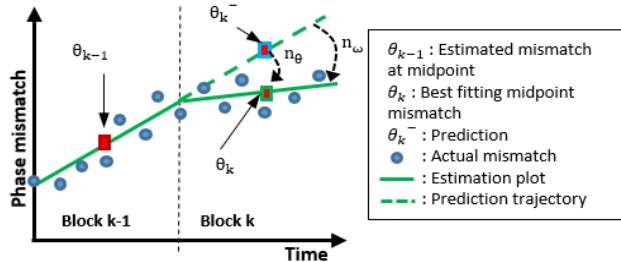


Fig. 1. Diagram showing the phase tracking concept of the parallelized schemes.

The Kalman filters are prediction-update type of estimators where a prediction of the state parameter vector x_k is done at time instance $k-1$ given as x_k^- . Using x_k^- , a prediction of the measurement at time k , y_k^- is calculated. In the next step we reach time instance k and make the actual measurement y_k . The final estimate of the Kalman filter at time instance k is then calculated using $x_k^+ = x_k^- + K_k (y_k - y_k^-)$, where K_k is the Kalman gain. The filter is said to be locked to the changes in state parameters when the prediction ($x_k^+ - x_k^-$) approaches zero. This can be achieved by minimizing ($y_k - y_k^-$).

In case of the LKF proposed in [11], it is assumed that the state parameters are themselves the observations i.e. $y_k = [\theta_k \ \omega_k]^T$. Thus, it is assumed that the actual phase mismatch at the midpoint of the block can be accurately inferred from measurements, which may not be strictly true. Moreover, the amplitude noise in the observed signal is not considered, further perturbing the measurement. To address these problems, we propose a new observation model (Eq. 4) that uses a complex observation noise (n_y) as opposed to the scalar observation noise (n_θ) used in the LKF.

$$\tilde{y}_k = e^{j\theta_k} + n_y \quad \text{and} \quad \tilde{\omega}_k = \omega_k + n_\omega \quad (4)$$

where n_y is a complex observation noise (incorporating both phase, n_θ and amplitude noise, n_a), as shown in Fig. 2. Moreover, the parameter \tilde{y}_k is the directly measured received sample at the midpoint of k^{th} block, stripped of its modulation by a slicer as shown in Fig. 2(c),

as opposed to $\tilde{\theta}_k$ which is inferred from measurements in [11]. The inclusion of the complex term n_y allows for correction of both amplitude and phase variations, and so is key to improving system performance at lower OSNRs. However, since the observation model is now non-linear, a LKF can no longer be used, and thus we use an unscented Kalman filter (UKF) [9]. While LKFs propagate predictions of the mean and variance of the state parameters through the observation model to update the Kalman filter [11], a UKF instead uses a set of ‘sigma points’ [9] that are specifically chosen to capture the statistical moments (and hence the probability distribution function) of the state parameters x_k , and are then propagated through the observation model. The mean and variance of these propagated sigma points are then used to update the Kalman filter. In addition to the changes to the observation model shown in Eq. 2 and 4, we also modify the state update equations as

$$\theta_{k+1} = N \cdot \omega_k + \theta_k + n_j \quad \text{and} \quad \omega_{k+1} = \omega_k + n_f \quad (5)$$

Here, adding n_j attempts to improve the state update by including a term for laser phase noise.

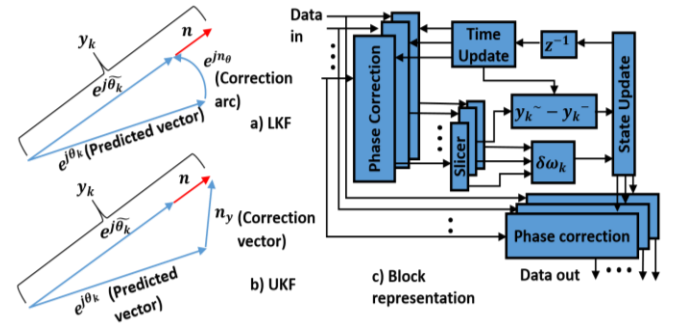


Fig. 2. Graphical representations of: (a) Linear Kalman Filter and (b) Unscented Kalman filter. n_a : amplitude noise vector, $e^{j\theta_k}$: Vector due to CFO, TO and PN.

Fig. 2 shows a graphical representation of the corrections that the linear and unscented Kalman filters apply and the block representation of the UKF, that is similar to that in [11] except for the calculation of ($y_k^- - y_k^-$) instead of $\delta\theta_k$ in LKF. If the received signal is stripped of its modulation, the residual component is of the form $y_k = e^{j\theta_k} + n$. When using a LKF, the observation model is given by Eq. (2). The LKF attempts to minimize the arc n_θ , and so instead of trying to approach y_k , it tries to approach $e^{j\theta_k^-}$ by minimizing the phase difference n_θ . The UKF attempts to minimize the vector n_y to approach y_k in Fig. 2b, which gives a more accurate estimate of the mismatch. For the UKF, the Kalman gain of UKF is a complex value, giving a phase shift as well as scaling. We compare the performance of the UKF to the LKF in the next section. We note that a similar state space model was proposed recently in [13] which uses an ‘extended’ Kalman filter (EKF) implementation. The inherent benefits of the UKF over EKF [9] predict that our UKF to provide higher system performance than an EKF.

The proposed system was verified experimentally in back-to-back configuration and over an 800-km optical fiber transmission link. A 10-Gbaud single-carrier signal was fed from arbitrary waveform generator (AWG) into a 20-GHz optical bandwidth IQ modulator that modulates the CW optical beam from a tunable laser (<100 kHz linewidth) set to 193.1 THz carrier frequency. A laser with same linewidth properties is used as a local oscillator at the receiver. In the case of back-to-back configuration, the amplified signal was fed to a 25-GHz electrical bandwidth integrated coherent receiver after optical noise loading. The noise loading setup consists of an EDFA with no input as an ASE source, a band-pass filter constraining the noise bandwidth to 200 GHz, and a second EDFA to boost the noise power. The optical noise is coupled with the optical signal with a 3-dB coupler. The coupled noise power, and thus the OSNR, is controlled with help of

a variable attenuator. For the link configuration, the optical signal was passed through 10 spools of optical fiber, each of length 80 km. Launch power was controlled by EDFAs placed before each spool, with a final EDFA placed as a pre-amplifier before the receiver. The amplified signal is filtered before the receiver using a BPF with bandwidth centered at the set transmission wavelength. The outputs of the coherent receiver digitized by a 40-GSa/s, 16-GHz bandwidth real-time oscilloscope. The digital signal processing algorithms of proposed system were run offline.

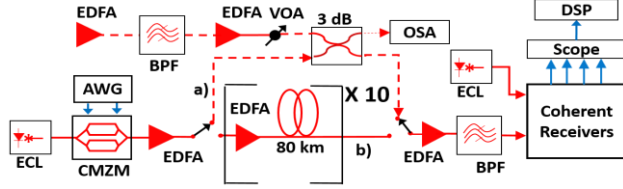


Fig. 3. Experimental setup in: (a) back-to-back configuration (b) 800-km transmission link configuration. BPF: Band pass filter, VOA: Variable optical attenuator, CMZM: Complex Mach-Zehnder modulator, AWG: Arbitrary waveform generator, ECL: External cavity laser.

For demonstrating a QPSK signal, we generate a 10-Gbaud modulated signal and receive in a back-to-back setup as shown in Fig. 3. The parallelized UKF and the parallelized LKF algorithms were implemented and the Q factor of the recovered constellation was calculated for each algorithm. We calculate Q from SNR as $Q = 10\log_{10}(SNR_{rec})$ where SNR_{rec} is the signal-to-noise ratio of the received signal at the output of the carrier recovery algorithm. At lower OSNRs, where the bit errors are reliably measurable, Q from the SNR matches with the Q from BER; i.e. $Q_{SNR} = Q_{BER}$, where Q_{BER} for M-QAM is given as

$$Q_{BER} = 20\log_{10}\left(\sqrt{\frac{2(M-1)}{3}} \times \operatorname{erfc}^{-1}\left(\frac{BER \times \log_2 \sqrt{M}}{1 - \frac{1}{\sqrt{M}}}\right)\right) \quad (6)$$

The Q factor for QPSK modulated signal in a back-to-back setup is plotted in Fig. 4 with OSNR sweep. Figs. 4a, 4b and 4c show the Q factor plots for the block lengths of 44, 142 and 198 respectively, demonstrating that the UKF performs better than the LKF, with less improvement at higher OSNRs. At low OSNRs the use of more accurate observation model, combined with the use of sigma points—more accurately capturing the signal pdf and the statistical moments of the state parameters—provides a performance advantage for the UKF over the LKF. As the OSNR increases, the amplitude noise vector in Fig. 2 reduces in magnitude relative to the signal vector. As such, the correction vector of the UKF approaches the correction arc of the LKF, resulting in the algorithms providing similar performance. At the FEC limit ($Q = 8.6$ dB, $BER = 3.8 \times 10^{-3}$), the UKF gives 1.2-dB, 1.5-dB and 2-dB improvement in required OSNR over the LKF for block lengths 44, 142 and 198, respectively. At optimum block length (44 samples), the UKF gives an implementation penalty of 0.3 dB, whereas it increases to 1.5 dB in case of LKF.

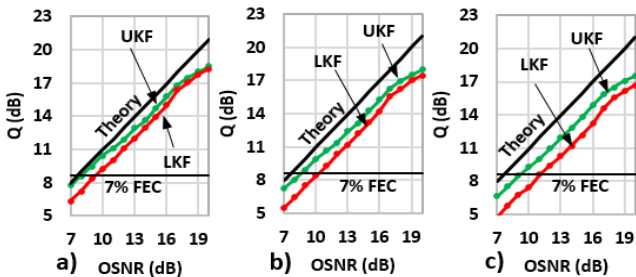


Fig. 4. Q vs. OSNR, block lengths of: (a) 44 (b) 142 and (c) 198 samples.

To investigate the effects of block length size on system performance, we sweep block length for a fixed received OSNR of 10 dB. Fig. 5a shows that Q reaches an optimum for block lengths of 44 samples and then steadily reduces with increases in block length. Compared with the measured Q performance when using the optimal block length, the block lengths 142 samples and 198 samples give Q penalties of 0.5 dB and 1 dB respectively. Block lengths below the optimum, where there are not enough samples to properly estimate the slope of the phase mismatch trajectory, causes reduction in Q . For longer blocks, the slope of the phase mismatch can vary considerably within a block, again giving rise to errors and reduction in Q as seen in Fig. 5a.

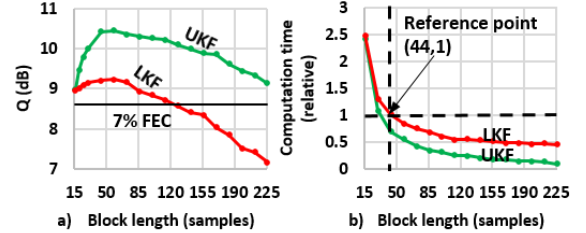


Fig 5. a) Q -value vs. block length, OSNR = 10 dB. b) Computation time in reference to that of LKF at block length = 44.

One of the factors that affects the computation time required to process a given number of symbols is the block length chosen. Fig. 5b shows the computation time with increasing block length in reference to that required by the parallelized LKF at optimum block length 44. Comparing Fig. 5a to 5b, the UKF not only gives a gain in Q but also consumes less computation time compared with the parallelized LKF. The computation gain comes from the extra N addition operations required by the LKF in order to calculate the prediction error for phase mismatch for k^{th} block ($\delta\theta_k$), that is used to update the state parameter vector x_k [11]. Since the phase mismatch is not directly observable from the received signal, the LKF calculates the error vector from mean of phase errors that requires N addition operations. When implementing an UKF, these N addition operations are avoided since the observations in this case are the received signal samples stripped of their modulation (y_k), and not the phase mismatch.

Another factor that should be considered in the computation time comparison between the LKF and UKF is the calculation of the sigma points in an UKF, which increases the number of operations. As the sigma points are independent of one-another, it is possible to parallelize their calculations; whereas the parallelization of the N addition operations required for the LKF is not possible. Thus, the UKF reduces the latency in the system, at the cost of more hardware. This is verified in the Fig. 5b where it can be seen that the total required computation time is reduced by 1.7 times that of parallelized LKF with an optimal block length. This computational benefit of UKF over LKF is possible only in case of parallelized architectures, not in the conventional serial architecture. As shown in Fig. 5, if the Q -value is sacrificed to certain extent, a considerable reduction in the computation time can be achieved. By increasing the block length from 44 to 142, we sacrifice 0.5-dB in Q but reduce the computation time to 30% that of block length 44. Similarly, if the block length is further increased to 198, the reduction in computation time reaches 20% that of block length 44 with reduction in Q of 1-dB.

Recent optical communication systems implement high-order modulation formats to increase spectral efficiency. As an example, 16-QAM is being investigated as a candidate modulation format for 400G optical transport [12]. Hence, we additionally look into a system using 16-QAM to verify that the UKF and LKF can be generalized to higher-order spectrally-efficient modulation formats. A 10-Gbaud 16-QAM modulated signal was generated and recovered using the two parallelized Kalman filter algorithms. In order to adapt the system to

higher-order modulation formats, only the demodulation block is changed that makes them attractive for modulation-format flexible transceivers.

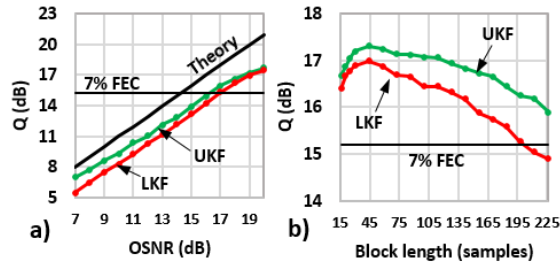


Fig. 6.a) Q vs. OSNR for 16-QAM, block length = 44; b) Q vs. block length for 16-QAM, OSNR = 19 dB.

Fig. 6a plots Q against received OSNR after using UKF and LKF on a 16-QAM signal taking 44-sample blocks. Similar to the QPSK case, the UKF gives higher performance gain at lower OSNRs than at higher OSNRs. However, in 16-QAM case, the improvement in required OSNR at 7% hard FEC limit ($Q=15.2$) reduces to 0.8-dB and the implementation penalty increases to 2-dB for UKF and 2.8-dB for LKF. The higher implementation penalty is as expected for 16-QAM over QPSK, and the smaller performance difference between the two Kalman filter implementations is expected at higher OSNRs (cf. Fig. 4).

By varying the block length at OSNR 19-dB, Q was again measured to be optimum at the block length of 44 samples. Thus, comparing the results for QPSK and 16-QAM systems, the proposed system shows similar trends independent of the modulation format, but at the same time, the performance gain for UKF over LKF reduces for higher QAM modulation formats at OSNRs required to keep Q above the FEC limit. Overall, although the performance gain in using an UKF over an LKF at optimized block length is not very large for both modulation cases, the improvement in computation time moving from an LKF to a UKF implementation is considerable. So, toward the goal of real-time implementation as desired in [11], the UKF may prove to be the lower latency option for processing either QPSK or 16-QAM signals.

The signal was transferred over an 800-km fiber link with varying launch powers to understand the effects fiber non-linearity. Fig. 7 plots the Q -values of the algorithms under test using a 44-sample block length, for QPSK and 16-QAM signals, with the launch power varied.

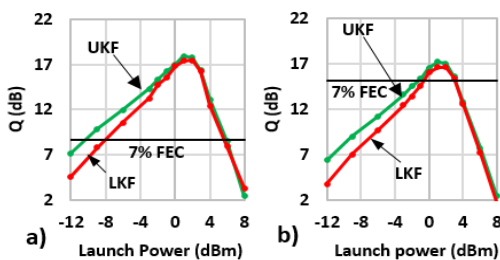


Fig. 7. Q vs. launch power for a) QPSK and b) 16-QAM, over an 800-km optical fiber link, using optimal block length.

At higher launch powers, the UKF and LKF performed similarly since neither is able to compensate for degradations of optical non-linear effects. Although the UKF gave 2.3-dBm improvement for QPSK case in the required launch power over the parallelized LKF at the FEC limit, this improvement was observed to be marginal (0.3-dBm) for 16-QAM case. It may be possible that the improvement in required launch power at the FEC limit can be increased for higher QAM modulation schemes by using soft decision forward error correction (SD-FEC), resulting in UKF providing an overall improvement in terms of reach in long haul systems and spectral efficiency with higher QAM modulation schemes. This remains to be investigated. Regardless of the peak

performance, the computation time of parallelized UKF is still 60% that of parallelized LKF. As such, the real advantage of using a parallelized UKF may be in reduced latency.

In conclusion, we have proposed a blind, unscented Kalman filter implementing a parallelized architecture for carrier recovery in single-carrier optical systems and compared the performance with previously proposed parallelized LKF. For block lengths optimized for Q performance, the UKF reduces the computation time by 1.7 times than that of parallelized LKF and requires 1.2-dB and 0.8-dB lower OSNR at the 7% hard FEC limit compared to the LKF for both QPSK and 16-QAM modulated signals respectively. These improvements in computation time and required OSNR were observed to be better for longer blocks. The proposed system was verified to perform successfully over an 800-km long-haul link, where the UKF gives 2.3-dBm improvement in the required launch power at hard FEC limit over LKF that reduces with the order of modulation. This study shows that in the case of parallelized architectures, for specific applications of carrier recovery in optical communication systems, an unscented Kalman filter can prove to be a better option than a linear Kalman filter.

Funding: Australian Research Council's Centre of Excellence (CUDOS) (CE110001018) and Laureate Fellowship (FL130100041) schemes.

Acknowledgement: We acknowledge the support from VPIphotonics (www.vpiphotonics.com) under their University Program.

References

1. M. Nakazawa, K. Kikuchi and T. Miyazaki, High spectral density optical communication technologies, Volume 6, (Springer-Verlag Berlin 2010).
2. S. J. Savory, Opt. Express **16**(2), p. 804 (2008).
3. I. Fatadin, D. Ives, S. J. Savory, Opt. Express **21**(8), p. 10166 (2013).
4. M. G. Taylor, J. Lightwave Technol. **27**(7), p. 901 (2009).
5. De Gaudenzi, T. Garde and V. Vanghi, J. Comm. IEEE Trans. **43**(12), p. 3090 (1995).
6. Timo Pfau, Sebastian Hoffman and Reinhold Noe, J. Lightwave Technol. **27**(8), p. 989 (2009).
7. M. G. Taylor, in Optical Fiber Communication Conference and Exposition (OFC) (2010) (Optical Society of America), San Diego, CA, USA, paper OThL4.
8. Donghe Zhao, Lixia Xi, Xianfeng Tang, Wenbo Zhang, Yaojun Qiao and Xiaoguang Zhang, Opt. Express **23**(19), p. 24822 (2015).
9. Eric A. Wan and Rudolph van der Merwe, Proc. IEEE Adaptive Systems for Signal Processing, Communications, and Control Symposium Conference (2000), Alberta, Canada, p. 153.
10. Steven Kay, Fundamentals of statistical signal processing, Volume 1: Estimation Theory, (Wiley 1993).
11. Takashi Inoue and Shu Namiki, Opt Express **22**(13), p. 15376 (2014).
12. OIF-Tech-Options-400G-01.0 –Technology Options for 400G Implementation (July 2015) (White paper).
13. Lalitha Pakala and Bernhard Schmauss, Opt Express **24**(6), p.6391 (2016).

References

1. M. Nakazawa, K. Kikuchi and T. Miyazaki, High spectral density optical communication technologies, Volume 6, (Springer-Verlag Berlin Heidelberg 2010).
2. Seb .J. Savory, "Digital filters for coherent optical receivers," *Opt. Express* **16**(2), p. 804-817 (2008).
3. I. Fatadin, D. Ives, S. J. Savory, "Differential carrier phase recovery for QPSK optical coherent systems with integrated tunable lasers," *Opt. Express* **21**(8), p. 10166-10171 (2013).
4. M. G. Taylor, "Phase estimation methods for optical coherent detection using digital signal processing," *J. Lightwave Technol.* **27**(7), p. 901-914 (2009).
5. De Gaudenzi, T. Garde and V. Vanghi, "Performance analysis of decision-directed maximum likelihood phase estimators for M-PSK modulated signals," *J. Comm. IEEE Trans.* **43**(12), p. 3090 (1995).
6. Timo Pfau, Sebastian Hoffman and Reinhold Noe, "Hardware-efficient coherent digital receiver concept with feedforward carrier recovery for M-QAM Constellations," *J. Lightwave Technol.* **27**(8), p. 989-999 (2009).
7. M. G. Taylor, "Algorithms for coherent detection," in *Optical Fiber Communication Conference and Exposition (OFC) and National Fiber Optic Engineers Conference (NFOEC)* (2010) (Optical Society of America), San Diego, CA, USA, paper OThL4.
8. Donghe Zhao, Lixia Xi, Xianfeng Tang, Wenbo Zhang, Yaojun Qiao and Xiaoguang Zhang, "Digital pilot aided carrier frequency offset estimation for coherent optical transmission system," *Opt. Express* **23**(19), p. 24822-24832 (2015).
9. Eric A. Wan and Rudolph van der Merwe, "The unscented Kalman filter for nonlinear estimation," *Proceedings of IEEE Adaptive Systems for Signal Processing, Communications, and Control Symposium Conference* (2000), Alberta, Canada, p. 153-158.
10. Steven Kay, *Fundamentals of statistical signal processing, Volume 1: Estimation Theory*, (Wiley 1993).
11. Takashi Inoue and Shu Namiki, "Carrier recovery for M-QAM signals based on a block estimation process with Kalman filter," *Opt Express* **22**(13), p. 15376-15387 (2014).
12. OIF-Tech-Options-400G-01.0 – Technology Options for 400G Implementation (July 2015) (White paper).
13. Lalitha Pakala and Bernhard Schmauss, "Extended Kalman filtering for joint mitigation of phase and amplitude noise in coherent QAM systems," *Opt Express* **24**(6), p.6391 (2016).